

Quantum confinement effects on the electronic structure of Si(001) ultrathin films: Energy shifts of optical band edges and luminescence in crystalline and amorphous Si films

Masahiko Nishida

Department of Physics, Kanazawa Institute of Technology, Nonoichi-machi, Ishikawa 921-8812, Japan

(Received 18 December 1998)

The electronic structure for Si(001) ultrathin films terminated by SiO₄ species is calculated by the extended Hückel-type nonorthogonal tight-binding method and compared to experimental results for amorphous Si(*a*-Si)/SiO₂ superlattices grown on (001)Si substrates by molecular beam epitaxy (MBE) [Lockwood *et al.*, Phys. Rev. Lett. **76**, 539 (1996)]. A remarkable coincidence in the energy shifts of the valence band maximum (VBM) and conduction band minimum (CBM) between the calculation and experiment strongly suggests that the MBE-grown *a*-Si well layers are almost crystalline and can have a CBM projected in the (001) growth direction and a local minimum of the conduction band as in the crystalline Si(001) films. The similarity of the thickness dependence of observed photoluminescence (PL) peak energy shifts to that of calculated energy-gap shifts indicates that the observed PL should be due to direct recombination of excitons between the VBM and the projected CBM of extended states quantized in the *a*-Si well layers as in the crystalline Si(001) ultrathin films. It is found that the binding energy of excitons (100 meV) related to the PL can be a combination of the increased Coulomb energy induced by a compression of wave functions for two-dimensional excitons and the one caused by a reduction in dielectric constant due to confinement in the growth direction. [S0163-1829(99)01123-6]

I. INTRODUCTION

Although a large amount of work has been done on the visible-light emission in Si quantum dots and wires,¹ there has been relatively little work on visible luminescence in two-dimensional ultrathin films of Si, because of their one-dimensional quantum confinement character. However, well-defined and controllable Si nanostructures such as two-dimensional ultrathin films are required for practical applications of band-gap engineering of quantum-confined structures that exhibit new optoelectronic phenomena that are absent in bulk Si.

Recently, well-characterized two-dimensional Si quantum wells and superlattices have been reported to provide room temperature photoluminescence (PL).²⁻⁶ Among others, Lockwood *et al.*² have reported visible light emission from amorphous-Si(*a*-Si)/SiO₂ superlattices, grown on (001)Si substrates by molecular beam epitaxy (MBE). They have shown that those highly luminescent superlattices exhibit clear quantum confinement shifts in the valence band maximum (VBM) and conduction band minimum (CBM) as well as PL peak energies with Si layer thickness. The observed results for PL are in striking contrast to those in conventional *a*-Si:H. No shift in PL due to quantum confinement has been reported in *a*-Si:H ultrathin layers, because of the occurrence of disorder-induced localized tail states.⁷

The fact that both the Si well layers and SiO₂ barrier layers in the Si/SiO₂ superlattices are amorphous is quite important, in the sense that amorphous materials are not restricted within lattice matching requirement at the interface in a quantum well heterostructure, in contrast to crystalline ones where a heterostructure must be prepared by two materials having the same or similar lattice constants. In fact, a large lattice mismatch at the interface between the crystal Si

(*c*-Si) and SiO₂ layers is likely to produce in-plane strain in *c*-Si wells and thus, *c*-Si/SiO₂ quantum wells exhibit PL peak energies almost independent of Si layer thickness,⁴⁻⁶ in contrast to the PL spectra in the *a*-Si/SiO₂ superlattices grown by MBE.² This suggests that atomic configurations at the interface between *c*-Si and SiO₂ are quite different from those between MBE-grown *a*-Si and SiO₂, resulting in different electronic structures at the interface and PL spectra. At present, however, detailed comparison is difficult, owing to the complicated difference in nature and structure of the related materials. The IR (infrared spectroscopy) confirmation that the MBE grown Si well layers in the *a*-Si/SiO₂ superlattices contain no significant amounts of hydrogen² is also important, because an upward shift in the optical band gap and PL in conventional *a*-Si:H can be correlated to higher hydrogen content in *a*-Si:H with smaller thickness by removing deepest localized states.⁸ For the reasons stated above, the amorphous Si well layers in the MBE-grown *a*-Si/SiO₂ superlattices seem to be quite different in nature from conventional *a*-Si or *a*-Si:H prepared by other methods such as glow discharge decomposition of SiH₄ and plasma enhanced chemical vapor deposition.

Very recently, tight-binding model calculations have been done for conventional ultrathin *a*-Si and *a*-Si:H layers with localized states, showing a substantial blueshift in energy gap due to confinement while failing to provide a definitive description of the experimentally observed PL energies.⁹ In addition, electronic structure calculations have been performed in the past for *c*-Si/SiO₂(001) superlattices¹⁰ and isolated oxygen-terminated Si(001) ultrathin films¹¹ by use of tight-binding methods, though both have not described any comparison of their calculated results with the experimental ones for the *a*-Si/SiO₂ superlattices deposited by MBE.²

In the present work, the electronic structure for crystalline

Si(001) ultrathin films terminated by SiO_4 species has been calculated and compared to the experimental results for the $a\text{-Si/SiO}_2$ superlattices grown on (001)Si substrates by MBE. The results show that the ultrathin layers of $a\text{-Si}$ in the superlattices can have the same kind of extended (delocalized) states as crystalline Si(001) ultrathin layers and provide convincing theoretical evidence for quantum confinement-induced luminescence due to direct transition of excitons between the optical band edges of extended states in the $a\text{-Si}$ well layers. Special emphasis is put on the analysis of energy shifts in the VBM and CBM and those in PL observed in the $a\text{-Si/SiO}_2$ superlattices. It is shown that electronic state calculations for the Si(001) ultrathin films terminated by SiO_4 species simulate sufficiently experimental results for the Si well layers in the $a\text{-Si/SiO}_2$ superlattices grown on (001)Si substrates by MBE.

II. MODEL AND CALCULATIONS

Electronic state calculations are carried out by applying the extended Hückel-type nonorthogonal tight-binding (EHNTB) method to the crystalline Si(001) ultrathin films or slabs. The detailed calculations of electronic structure and oscillator strength by the EHNTB method have been described in Ref. 11. Here, we briefly describe the EHNTB method. This is a non-self-consistent method of the two-center approximation. The basis consists of one s and three p orbitals centered on each atom. The energy matrix elements are proportional to the overlap matrix elements, which are calculated using Slater-type atomic orbitals which approximate atomic basis orbitals. All distant-neighbor nonorthogonal overlaps and interactions between basis orbitals up to the sixth ones are included explicitly. The EHNTB parameters for Si are determined by means of an accurate fit of the bulk band structure calculated using 5.43 \AA as a lattice constant to the empirical nonlocal-pseudopotential band structure for Si. The EHNTB parameters between H and Si and between H and H and those between O and Si and between O and O are determined by fitting calculated surface electronic states on the H- and O-covered Si(111) surfaces, which have been intensively studied, to experimental data.¹¹ It is noted that the EHNTB method does not use the effective mass approximation.

There are two surfaces on both sides of the films and the two-dimensional periodicity parallel to the film surface is preserved. In order to simulate the Si/SiO₂ interface, the films are terminated by SiO_4 surface species with silicon bonded to four oxygen atoms, as shown in Fig. 1(a) where the H-terminated configuration is also presented for geometrical comparison (the Si-H bond length is 1.48 \AA). Dangling bonds on the surface Si atoms are fully passivated by oxygen atoms in this configuration. The silicon atom in the SiO_4 tetrahedron species on the Si(001) films has topologically the same bond configuration as in SiO_2 . The Si-O bond length is taken as 1.64 \AA and the length between the two adjoining oxygen atoms at the topmost layer is taken to be 1.47 \AA as in the H_2O_2 molecule.¹² The bond angle of Si-O-Si is taken as 180° for the sake of simplicity.¹³ The SiO_4 -terminated configuration in the Si ultrathin films is found to be sufficient to simulate the interface in the $a\text{-Si/SiO}_2$ superlattices deposited by MBE. Figure 1(b) illus-

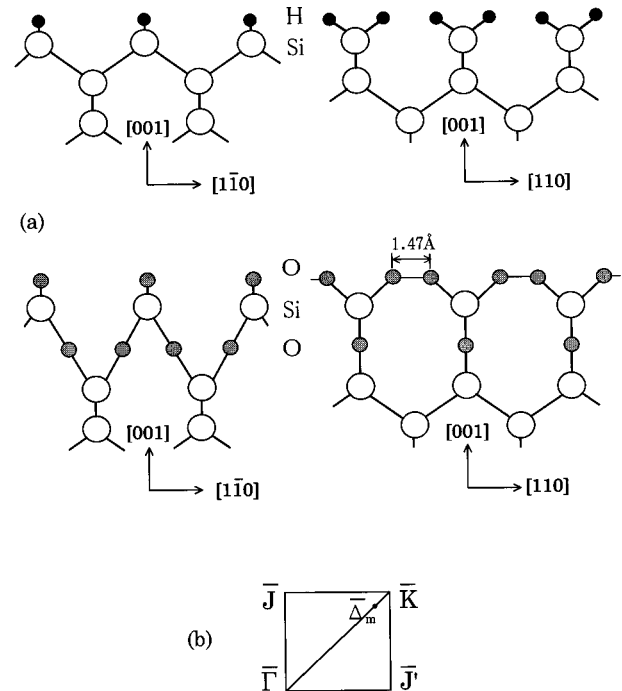


FIG. 1. (a) Side view of the SiO_4 -terminated Si(001) film configuration. The H-terminated configuration is also presented for geometrical comparison. The black, shaded, and open circles denote the hydrogen, oxygen, and silicon atoms, respectively. (b) The irreducible part of the surface Brillouin zone for the (001) film. The signs $\bar{\Gamma}$ and $\bar{\Delta}_m$ denote the zone center and the location where the bulk CBM occurs, respectively.

trates the irreducible part of the surface Brillouin zone (SBZ) for the (001) film. The signs $\bar{\Gamma}$ and $\bar{\Delta}_m$ denote the zone center and the location where the bulk CBM occurs, respectively. Dispersion relations of the valence and conduction bands are calculated along the symmetry directions in the SBZ. The energies (in eV) are referred to the VBM for Si films. Calculated results are reported for Si(001) ultrathin films with thickness ranging up to 44 Si atomic layers (about 6 nm in thickness).

III. RESULTS AND DISCUSSION

To gain insight, we first show in Fig. 2 the calculated energy dispersions of the valence and conduction band edges near the fundamental band gap along the symmetry directions in the SBZ. The result calculated for a SiO_4 -terminated Si(001) ultrathin film (solid lines) is compared to that for the H-terminated one (dotted lines). Here the number of Si layers in the film is six for both configurations. The VBM and CBM energies in the infinite Si bulk are shown by the horizontal dashed lines. The VBM's of the films for both configurations appear at the $\bar{\Gamma}$ point in the SBZ. On the other hand, the two bulk CBM's of Si along the [001] directions are projected onto the film surface and appear at the $\bar{\Gamma}$ point, and the other four bulk CBM's along the [100] and [010] directions occur at the $\bar{\Delta}_m$ point, as described in Ref. 11. According to effective mass theory, the projections at $\bar{\Gamma}$ are upshifted in energy by a small amount, because the heavy longitudinal mass controls the kinetic energy of confinement

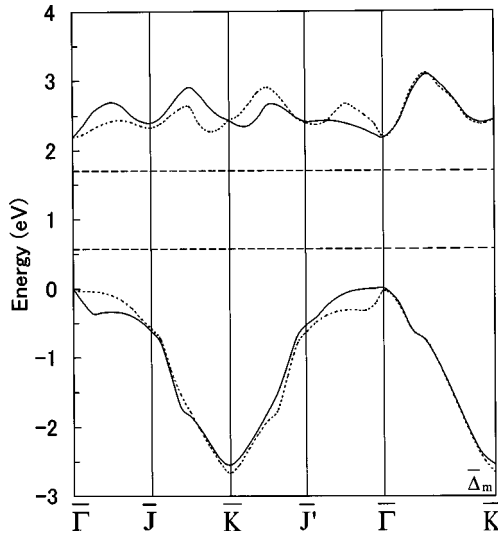


FIG. 2. Energy dispersion curves of the valence and conduction band edges for the SiO₄-terminated Si(001) ultrathin film (solid lines) in comparison with those for the H-terminated one (dotted lines). The number of Si layers in the film is 6. The VBM and CBM energies in the infinite Si bulk are shown by the horizontal dashed lines.

along the [001] direction, while the projections at $\bar{\Delta}_m$ are also upshifted in energy, but by a larger amount, because their energies are determined by the light transverse mass owing to confinement in the [001] direction. Therefore, the energy states projected at $\bar{\Gamma}$ are lower in energy than the projections at $\bar{\Delta}_m$. As a result, the energy states folded onto $\bar{\Gamma}$ form the CBM (referred to as the projected CBM) and those projected at $\bar{\Delta}_m$ are expected to be a local minimum of the conduction band (LMCB), in the Si(001) ultrathin films. This is the reason for the band gaps of the Si(001) ultrathin films being direct. The situation mentioned above can be seen in Fig. 2. The VBM's and CBM's at $\bar{\Gamma}$ and the LMCB's at $\bar{\Delta}_m$ of the films for both configurations are found to be shifted in energy from the VBM and CBM in the Si bulk owing to quantum size effects, as seen in Fig. 2. We notice that, aside from some slight difference in details of dispersion behavior, there is little difference in energy of the VBM and CBM at $\bar{\Gamma}$ as well as the LMCB at $\bar{\Delta}_m$ between the SiO₄- and H-terminated films with the same number of Si layers.

Figure 3 shows the calculated energy shifts of the VBM and CBM at $\bar{\Gamma}$ and of the LMCB at $\bar{\Delta}_m$ from the bulk values as a function of the number of Si layers in the films terminated by SiO₄ species (open and closed circles), in comparison with the H-terminated case (solid and dashed lines). It is seen that the VBM shifts down and the CBM and LMCB shift up from the bulk with the decrease in Si layer thickness, reflecting quantum confinement effects. The energies of the VBM, CBM, and LMCB for the film terminated by SiO₄ are almost the same as those for the H-terminated case in all Si films under study. This means that the energies of the VBM and CBM at $\bar{\Gamma}$ and the LMCB at $\bar{\Delta}_m$, and thus the direct ($\bar{\Gamma}_v - \bar{\Gamma}_c$) and indirect ($\bar{\Gamma}_v - \bar{\Delta}_{mc}$) band gaps for the films under study are determined through quantum confinement

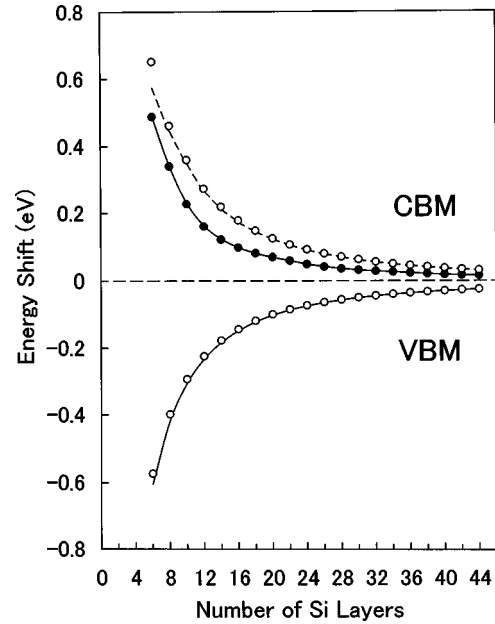


FIG. 3. Calculated energy shifts of the VBM and CBM at $\bar{\Gamma}$ and the LMCB (see the text) at $\bar{\Delta}_m$ from the bulk values as a function of the number of Si layers in the Si(001) ultrathin films terminated by SiO₄ species (open and closed circles), in comparison with those for the H-terminated case (solid and dashed curves). In the CBM section, the closed circles and solid curve denote the CBM at $\bar{\Gamma}$ and the open circles and dashed curve the LMCB at $\bar{\Delta}_m$.

only by the number of Si layers, i.e., the thickness of layers for the Si skeleton in the film, irrespective of the passivating species. This is because energy states associated with Si-O or Si-H on the surface occur far away from the fundamental band gap and no localized states appear around the band edges for both configurations.

On the other hand, the SiO₄ termination tends to intensify oscillator strength for the films. Figure 4 presents the calculated oscillator strength between the VBM and CBM (*y* polarization along the [110] direction) at the $\bar{\Gamma}$ point in the SBZ as a function of the number of Si layers for the Si(001) ultrathin films terminated by SiO₄ on both sides (squares), in comparison with the H-terminated case (*x* polarization along the $[1\bar{1}0]$ direction) (triangles). Electronic state calculations have been carried out for the films terminated by SiO₄ on one side and by H on the other side, in order to simulate partially passivated Si nanostructures. The circles in Fig. 4 show the resulting oscillator strength (*y* polarization). Although the calculated energy positions of the VBM, CBM, and LMCB, and thus the band gaps do not depend on the extent of passivation by SiO₄ species, the oscillator strength or possible luminescence intensity is enhanced by up to an order of magnitude with the increase in the amount of SiO₄ species passivating the films, reflecting an increase in the mixing between the projected CBM and the zone-center states due to the Si-O-Si bonds on the film surface.¹¹

In Fig. 5, the calculated energy shifts in the VBM and CBM at $\bar{\Gamma}$ and the LMCB at $\bar{\Delta}_m$ are replotted, respectively, by the solid lines and the dotted line from Fig. 3, for the purpose of comparing them to the experimental results (open symbols) for the *a*-Si/SiO₂ superlattices deposited on

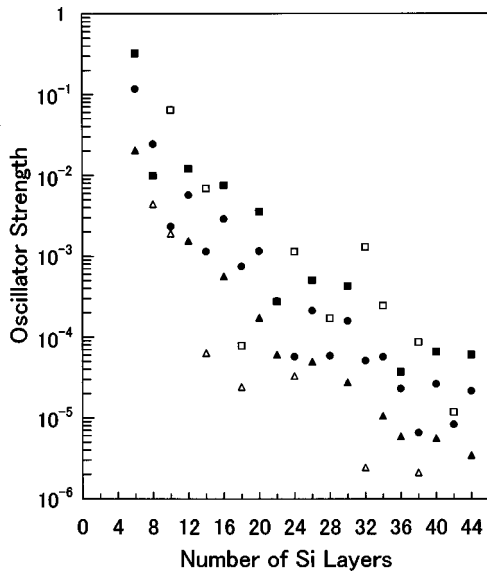


FIG. 4. Calculated oscillator strength between the VBM and CBM (y polarization along the $[110]$ direction) at the $\bar{\Gamma}$ point in the SBZ as a function of the number of Si layers for the Si(001) ultrathin films terminated by SiO₄ on both sides (squares) and for those terminated by SiO₄ on one side and by H on the other side (circles), in comparison with the H-terminated case (x polarization along the $[1\bar{1}0]$ direction) (triangles). The closed and open symbols refer to the lowest and second-lowest energy transitions, respectively.

(001)Si substrates by MBE.² Here, the calculated results are shown as a function of Si layer thickness (nm) for the sake of comparison with the experiment. The experimental VBM and CBM shifts have been determined by x-ray photoelectron spectroscopy and Si *L*-edge x-ray absorption spectroscopy, respectively, for MBE-grown (Si/SiO₂)₆ superlattices at room temperature.² It is noted that the measured points for

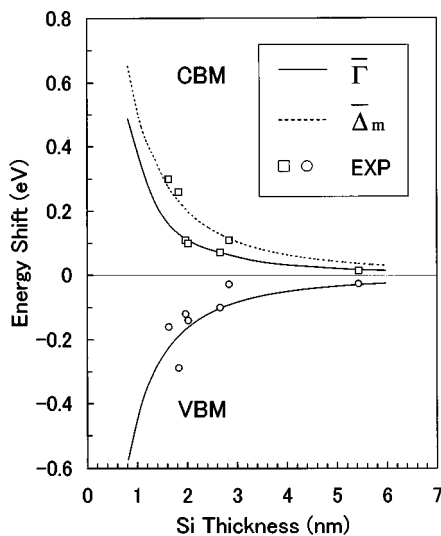


FIG. 5. Calculated energy shifts in the VBM and CBM at $\bar{\Gamma}$ and the LMCB (see the text) at $\bar{\Delta}_m$ are replotted, respectively, by the solid lines and the dotted line from Fig. 3 as a function of Si layer thickness (nm). The experimental results for the *a*-Si/SiO₂ superlattices deposited on (001)Si substrates by MBE (Ref. 2) are presented by the open symbols.

the superlattices are in remarkable agreement with the calculated curves for the crystalline films, suggesting that there is no trace of localized band-tail states observed above the VBM and those below the CBM. As clearly seen in Fig. 5, some of the observed points agree with the calculated curve for the CBM projected at $\bar{\Gamma}$ and others coincide with that for the LMCB at $\bar{\Delta}_m$ in the crystalline Si(001) ultrathin films. This implies that there can be two kinds of minimum of the conduction band in the MBE-grown *a*-Si well layers, as in the crystalline Si(001) films with the projected CBM and the LMCB. Therefore, it is quite likely that the core 2*p* electrons in the Si *L*-edge x-ray measurements for the *a*-Si/SiO₂ superlattices are excited to the CBM projected in the growth direction as well as to the LMCB in the *a*-Si well layers. Obviously, more detailed measurements need to be done for the VBM and CBM shifts in the *a*-Si/SiO₂ superlattices, in order to confirm the above description.

The fact that the shifts in the VBM and CBM observed in the MBE-grown *a*-Si/SiO₂ superlattices behave in the same way as those calculated for the crystalline Si(001) ultrathin films strongly suggests that both the VBM and CBM observed in the Si well layers of the MBE-grown superlattices are the same kind of extended (delocalized) states as those in crystalline Si films. This would be a manifestation of the fact that the intermediate as well as short-range order is very nearly the same in the MBE-grown *a*-Si and crystalline Si. As is well known, a quantum confinement effect would not be expected to occur in conventional *a*-Si:H with large disorder and the resulting small electron mean free path (~ 1 nm). However, quantum confinement effects on extended states in *a*-Si is expected to be similar to those in crystalline Si, as long as the coherence length of electron wave function in the delocalized states is long compared to the Si film or well layer thickness. The latter should be the reason for the striking coincidence in the energy shifts of the VBM and CBM between the experiment and calculation. The suggested presence of the projected CBM and the LMCB in the MBE-grown *a*-Si layers as in the crystalline Si films would be related to a recently reported assumption that the *a*-Si:H band gap is indirect, independent of local silicon bonding environments, as suggested by a model based on the interaction of electronic bands and a phonon band.¹⁴ Thus, the remarkable coincidence between the calculation and experiment strongly suggests that the amorphous Si well layers in the MBE-grown *a*-Si/SiO₂ superlattices are almost crystalline and have the same growth direction as the (001)Si substrate, and do not have any significant localized band-tail states, in contrast to the case of conventional *a*-Si:H.

Figure 6 shows the energy gap shifts from the bulk calculated for the SiO₄-terminated Si(001) ultrathin films as a function of Si film thickness (nm). The shifts in the direct ($\bar{\Gamma}_v - \bar{\Gamma}_c$) and indirect ($\bar{\Gamma}_v - \bar{\Delta}_{mc}$) band gaps are presented by the solid and dashed lines, respectively, in comparison with the shifts in PL peak energy from the bulk observed for the MBE-grown (Si/SiO₂)₆ superlattices at room temperature.² It is easily found that the calculated energy-gap shifts and the observed PL peak energy shifts are increasing in a similar way with decreasing Si layer thickness below 3 nm. Furthermore, it is worth noting that the shifts in band-gap energy calculated by the theory are systematically larger by a certain

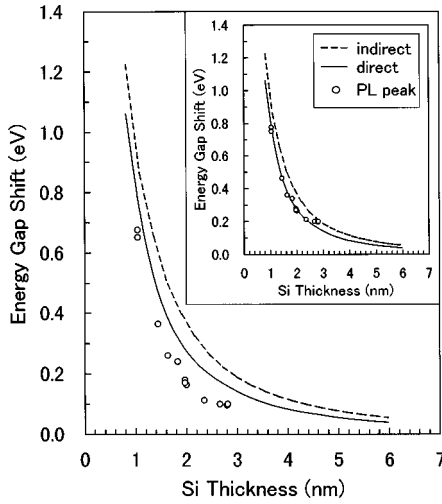


FIG. 6. Calculated shifts in energy gap from the bulk for the SiO_4 -terminated $\text{Si}(001)$ ultrathin films as a function of Si film thickness (nm). The solid and dashed lines show the shifts in the direct ($\bar{\Gamma}_v - \bar{\Gamma}_c$) and indirect ($\bar{\Gamma}_v - \bar{\Delta}_{mc}$) band gaps, respectively. The photoluminescence peak energy shifts from the bulk observed for the MBE-grown $(\text{Si}/\text{SiO}_2)_6$ superlattices at room temperature (Ref. 2) are also plotted for comparison and moved up in energy by 100 meV in the inset.

amount than those in experimental PL peak energy. We can find that the experimental PL peak energy shifts which are moved up by 100 meV coincide almost perfectly with the curve for the calculated shifts in the direct band gap at $\bar{\Gamma}$, as shown in the inset of Fig. 6. In addition, the increase in the calculated energy-gap shifts with decreasing Si layer thickness is also consistent with that in energy shifts of the first absorption edge observed in single a -Si:H ultrathin layers, though the confinement direction is unknown in the experiment.¹⁵

Now we examine the mechanism of the upward shift in the PL spectra observed for layer thickness below 3 nm. At first, we can preclude the possibility that an increase in optical band gap and PL peak energy is correlated to higher hydrogen content in a -Si with decreased thickness, because the MBE-grown a -Si materials under consideration are hydrogen free.² Thus, another mechanism must be at work. We consider quantum confinement as a source of the upward shift. The clear thickness dependence of the PL spectra would be much more unambiguous signal for quantum size effects than that of the optical band gap in amorphous structures, since optical band-gap measurements are not always adequate indicators of a quantum confinement effect for carriers in a -Si:H and the interpretation of usually reported blueshifts measured by conventional optical absorption spectroscopy in a -Si:H-related multilayers on the basis of quantum confinement is open to question.¹⁶

As stated above, no significant localized band-tail states are found to exist in the MBE-grown a -Si from the comparison of the energy shifts in the VBM and CBM measured using x-ray techniques with the calculated counterparts in the crystalline Si ultrathin films. If significant localized states are located in band tails near the VBM and/or CBM, photoexcited carriers quickly thermalize down to the band tails. Then, the lowest energy states in the band tails reached by

the holes and electrons before radiative recombination determine the energy of the PL emission as in conventional a -Si:H (~ 1.4 eV). In this situation, PL energy shifts due to quantum confinement would be negligible.⁷ Thus, judging from the experimental results for PL and their comparison with the calculated results, the PL should be based on the quantization of extended states in the MBE-grown a -Si layers, as insisted by Lockwood *et al.*,² in contrast to conventional a -Si:H where PL is due to localized tail states. The electron-hole transition will then occur between optical band edges of the extended states, i.e., between the VBM and CBM in the MBE-grown a -Si. Although the PL peak energy for a very large thickness (>3 nm) in the MBE-grown a -Si well layers is 1.6 eV and is larger than that in crystalline Si,² the shifts in PL peak energy are independent of whether the Si regions responsible for the light emission are amorphous or crystalline.

Finally we consider the implications of the energy difference (100 meV) between the observed shifts in PL peak energy and the calculated band-gap shifts for the Si layer thickness less than 3 nm. As mentioned above, we can assume that the PL is caused by direct recombination of excitons between optical band edges of extended states quantized in the a -Si well layers, which corresponds to the direct transition between the VBM and CBM at $\bar{\Gamma}$ in the crystalline $\text{Si}(001)$ ultrathin films. Then the energy difference stated above can be attributed to the binding energy of excitons confined in the ultrathin films. Here we refer to this energy difference of 100 meV as the experimentally observed binding energy of excitons.

On the other hand, excitonic behavior can be enhanced in the ultrathin films, because the physical separation between electron and hole is reduced in the confinement direction, as a result of which the Coulomb interaction increases. This will lead to an enhanced binding energy of excitons in the ultrathin films. In a one-dimensionally confined system such as Si ultrathin films, excitonic behavior should be two dimensional and the Coulomb interaction in the nonconfined directions parallel to the film surface predominates in excitonic effects. The binding energy for a purely two-dimensional exciton (flat exciton) in the ideal situation is enhanced at most up to four times the bulk value and given by¹⁷

$$E_B = 4R_y. \quad (1)$$

Here R_y is the effective Rydberg constant and

$$R_y = \frac{e^4 \mu}{32\pi^2 \hbar^2 \epsilon^2}, \quad (2)$$

where μ is the reduced mass along the film surface, e the electron charge, and ϵ the dielectric constant. The reduced mass along the film surface can be estimated by

$$\frac{1}{\mu} = \frac{1}{m_e} + \frac{1}{m_h}. \quad (3)$$

Here, we consider an electron lying in the CBM at $\bar{\Gamma}$ projected along the $[001]$ directions and thus m_e is taken to be the experimental transverse effective mass of electron in Si and $m_e = 0.19m_0$ where m_0 is the mass of free electron. On

the other hand, m_h at the VBM is taken as $0.54m_0$ which is the bulk effective mass for heavy hole in Si. The resulting reduced mass along the film surface is $\mu = 0.14m_0$.

When we take the dielectric constant ϵ for the Si ultrathin films to be 11.4 as in Si bulk, the calculated binding energy E_B is 58 meV, which is much smaller than the experimentally observed one. On the other hand, electrostatic screening in semiconductor nanostructures is expected to be different from its bulk counterpart. Theoretical studies on the dielectric constant in quantum confined systems have shown that significant drops in dielectric constant take place.^{18,19} The reduction in dielectric constant will lead to an increase in the binding energy of excitons. If we assume that the value of E_B in Eq. (1) is equal to 100 meV, the experimentally observed binding energy of excitons, then the resulting dielectric constant ϵ is estimated to be 8.74.²⁰ This value for the dielectric constant in the Si ultrathin films is in reasonable agreement in order of magnitude with the value of 8.18 for the dielectric constant in a Si quantum dot with 3 nm in diameter.¹⁸ Thus, we can say that the experimentally observed binding energy of excitons in the Si well layers in the a -Si/SiO₂ superlattices with the Si layer thickness below 3 nm is a combination of the increased Coulomb energy induced by a compression of wave functions for two-dimensional excitons and the one caused by a reduction in dielectric screening due to confinement.

IV. CONCLUSIONS

The electronic structure for the crystalline Si(001) ultrathin films terminated by SiO₄ species has been calculated by the EHNTB method and compared to the experimental results for the a -Si/SiO₂ superlattices grown on (001)Si substrates by MBE. Special emphasis has been put on the similarity of energy shifts in the VBM and CBM between the Si well layers in the superlattices and the crystalline Si(001)

ultrathin films terminated by SiO₄ species and on the correlation of the observed PL spectra and the calculated band gaps. The results are summarized as follows.

(1) Although the calculated energy positions of the VBM, CBM, and LMCB and thus the calculated band gaps do not depend on the species terminating the Si films under study nor on the extent of the passivation of the films by SiO₄ species, the calculated oscillator strength is enhanced by factors of up to 10 with the increase in the amount of SiO₄ species passivating the Si films.

(2) The remarkable coincidence in the energy shifts of the VBM and CBM between the calculation and experiment strongly suggests that the Si well layers in the MBE-grown a -Si/SiO₂ superlattices are almost crystalline and can have the CBM projected in the same growth direction as in the (001)Si substrates and the LMCB as in the crystalline Si(001) films.

(3) The similarity of the thickness dependence of the observed PL peak energy shifts to that of the calculated energy-gap shifts indicates that the PL should not be related to localized tail states as in conventional a -Si:H, but due to direct recombination of excitons between the VBM and projected CBM of extended states quantized in the a -Si well layers, which corresponds to the direct transition between the VBM and CBM at $\bar{\Gamma}$ in the crystalline Si(001) ultrathin films.

(4) The experimentally observed binding energy of excitons (100 meV) in the Si well layers in the superlattices with Si layer thickness below 3 nm can be a combination of the increased Coulomb energy induced by a compression of wave functions for two-dimensional excitons and the one caused by a reduction in dielectric constant due to confinement in the growth direction.

To conclude, the electronic states calculated for the Si(001) ultrathin films terminated by SiO₄ species simulate sufficiently those for the Si well layers in the a -Si/SiO₂ superlattices grown on (001)Si substrates by MBE.

¹A. G. Cullis, L. T. Canham, and P. D. J. Calcott, *J. Appl. Phys.* **82**, 909 (1997).

²D. J. Lockwood, Z. H. Lu, and J. M. Baribeau, *Phys. Rev. Lett.* **76**, 539 (1996).

³R. Tsu, J. Morais, and A. Bowhill, in *Microcrystalline and Nanocrystalline Semiconductors*, edited by L. Brus, M. Hirose, R. W. Collins, F. Koch, and C. C. Tsai, MRS Symposia Proceedings No. 358 (Materials Research Society, Pittsburgh, 1995), p. 825; D. A. Grützmacher, E. F. Steigmeier, H. Auderset, R. Morf, B. Delley, and R. Wessicken, *ibid.*, p. 833; L. Vervoort, F. Bassani, I. Mihalcescu, J. C. Vial, and F. A. d'Avitaya, *Phys. Status Solidi B* **190**, 123 (1995).

⁴Y. Takahashi, T. Furuta, Y. Ono, T. Ishiyama, and M. Tabe, *Jpn. J. Appl. Phys., Part 1* **34**, 950 (1995).

⁵P. N. Saeta and A. C. Gallagher, *Phys. Rev. B* **55**, 4563 (1997).

⁶S. Okamoto and Y. Kanemitsu, *Solid State Commun.* **103**, 573 (1997); Y. Kanemitsu and S. Okamoto, *Phys. Rev. B* **56**, R15 561 (1997).

⁷H. Munekata and H. Kukimoto, *Jpn. J. Appl. Phys., Part 2* **22**, L544 (1983); *J. Non-Cryst. Solids* **59/60**, 1167 (1983).

⁸B. A. Wilson, C. M. Taylor, and J. P. Harbison, *Phys. Rev. B* **34**, 4429 (1986); **34**, 8733 (1986).

⁹G. Allan, C. Delerue, and M. Lannoo, *Appl. Phys. Lett.* **71**, 1189 (1997).

¹⁰N. Tit and M. W. C. Dharma-wardana, *Solid State Commun.* **106**, 121 (1998).

¹¹M. Nishida, *Phys. Rev. B* **58**, 7103 (1998).

¹²A. F. Wells, *Structural Inorganic Chemistry* (Clarendon, Oxford, 1975), p. 420.

¹³Calculations have been performed for the Si-O-Si bond angle ranging from 180° - 40° to 180° + 40° and have found that main conclusions presented here are not changed at all.

¹⁴C. M. Fortmann, *Phys. Rev. Lett.* **81**, 3683 (1998).

¹⁵K. Hattori, T. Mori, H. Okamoto, and Y. Hamakawa, *Appl. Phys. Lett.* **53**, 2170 (1988).

¹⁶M. Beaudoin, M. Meunier, and C. J. Arsenaault, *Phys. Rev. B* **47**, 2197 (1993).

¹⁷M. Shinada and S. Sugano, *J. Phys. Soc. Jpn.* **21**, 1936 (1966).

¹⁸R. Tsu, L. Ioriatti, J. F. Harvey, H. Shen, and R. A. Lux, in *Microcrystalline and Nanocrystalline Semiconductors*, edited by L. Brus, M. Hirose, R. W. Collins, F. Koch, and C. C. Tsai, MRS Symposia Proceedings No. 283 (Materials Research Society, Pittsburgh, 1993), p. 437; R. Tsu and D. Babic, in *Optical*

- Properties of Low Dimensional Silicon Structures*, edited by D. C. Bensahel, L. T. Canham, and S. Ossicini, NATO Advanced Study Institute Series B: Physics (Kluwer Academic Publishers, Dordrecht, 1993), p. 203.
- ¹⁹R. Tsu and L. Ioriatti, *Superlattices Microstruct.* **1**, 295 (1985); L. W. Wang and A. Zunger, *Phys. Rev. Lett.* **73**, 1039 (1994); M. Lannoo, C. Delerue, and G. Allan, *ibid.* **74**, 3415 (1995).
- ²⁰The effective Bohr radius is $a_0 = 4\pi\epsilon\hbar^2/e^2\mu$ in bulk. The Bohr radius of a two-dimensional flat exciton $a_B = a_0/2$, which is estimated to be 1.65 nm for the Si layers under study, using $\epsilon = 8.74$.